REPORT DOCUMENTATION PAGE

AFRL-SR-AR-TR-04-

0167

1. REPORT DATE (DD-MM-YYYY)	2. REPORT TYPE	3. DATES COVERED (From - To)
09-03-2004	Final	15-06-2001 to 30-09-2003

4. TITLE AND SUBTITLE
Impact of External, Wall, and Pressure-Gradient Conditions on Overlap Region Parameters in High Reynolds Number Boundary Layers

5a. CONTRACT NUMBER

5b. GRANT NUMBER
F49620-01-1-0445

5c. PROGRAM ELEMENT NUMBER
61102F

6. AUTHOR(S)
Hassan M. Nagib

5d. PROJECT NUMBER
2307

5e. TASK NUMBER
BX

5f. WORK UNIT NUMBER

7. PERFORMING ORGANIZATION NAME(S) AND ADDRESS(ES)

Illinois Institute of
Technology
3300 S. Federal Street
Chicago, IL 60616-3793

8. PERFORMING ORGANIZATION REPORT NUMBER

9. SPONSORING / MONITORING AGENCY NAME(S) AND ADDRESS(ES)
USAF, AFRL
AF Office of Scientific Res
4015 Wilson Blvd., Room 713
Arlington, VA 22203-1954

NA

10. SPONSOR/MONITOR'S ACRONYM(S)

11. SPONSOR/MONITOR'S REPORT NUMBER(S)

12. DISTRIBUTION / AVAILABILITY STATEMENT

Approved for public release, Distribution is unlimited

20040319 110

13. SUPPLEMENTARY NOTES

14. ABSTRACT

In Part I of our work, mean velocity distributions in the overlap region, over the range of Reynolds, numbers $10,000 < Re_\theta < 70,000$, under five different pressure-gradient conditions are accurately described by a log law. The pressure-gradient conditions include adverse, zero, favorable, strongly favorable, and a complex condition. Parameters of the logarithmic overlap region developed from these higher Reynolds number boundary layers remain independent of Reynolds number when the boundary layers are under equilibrium conditions. The best estimate of the log-law parameters from the zero-pressure gradient boundary layers is $\kappa = 0.37$, $B = 4.0$. In Park II of our work a three-dimensional turbulent boundary layer over a flat plate is carefully documented with SPIV. At the first measurement station, the boundary layer is nearly two-dimensional before the secondary flow is generated via removal of mass through the side wall of the test section. The measurements are contrasted with Computations made using the commercial code by FLUENT.

15. SUBJECT TERMS

16. SECURITY CLASSIFICATION OF: U			17. LIMITATION OF ABSTRACT	18. NUMBER OF PAGES	19a. NAME OF RESPONSIBLE PERSON
a. REPORT	b. ABSTRACT	c. THIS PAGE			Mary Spina
U	U	U		10	19b. TELEPHONE NUMBER (include area code) (312) 567-3035

IMPACT OF EXTERNAL, WALL, AND PRESSURE-GRADIENT CONDITIONS ON OVERLAP REGION PARAMETERS IN HIGH REYNOLDS NUMBER BOUNDARY LAYERS

Hassan M. Nagib
Mechanical, Materials and Aerospace Engineering Department
Illinois Institute of Technology, Chicago, IL 60616

Abstract

In *Part I* of our work, mean velocity distributions in the overlap region, over the range of Reynolds numbers $10{,}000 < Re_\theta < 70{,}000$, under five different pressure-gradient conditions are accurately described by a log law. The pressure-gradient conditions include adverse, zero, favorable, strongly favorable, and a complex condition. The wall-shear stress was measured using oil-film interferometry, and hot-wire sensors were used to measure velocity profiles. Parameters of the logarithmic overlap region developed from these higher Reynolds number boundary layers continue to be consistent with our recent findings and to remain independent of Reynolds number when the boundary layers are under equilibrium conditions. The best estimate of the log-law parameters from the zero-pressure gradient boundary layers is $\kappa = 0.37$, $B = 4.0$. However, the Kármán "coefficient" (κ) is found to vary considerably for the non-equilibrium boundary layers under the various pressure gradients. The results highlight the variation with pressure gradient not only in the outer region of the boundary layer but also within the inner region.

In addition, in *Part II* of our work a three-dimensional turbulent boundary layer over a flat plate is carefully documented with SPIV. At the first measurement station, the boundary layer is nearly two-dimensional before the secondary flow is generated via removal of mass through the side wall of the test section. Subsequently, the layer is subject to an adverse pressure gradient due to turning of the initially two-dimensional flow. The wall shear-stress vector and its direction are measured directly using oil-film interferometry. The results indicate that the TKE increases slightly, mainly through changes in $u'u'$. The Reynolds stresses are all affected by the mean flow three-dimensionality with turbulence production and the pressure-rate-of-strain tensor playing the major role in the dynamics of the Reynolds stresses. Measurements of Townsend's structure parameter indicate that it is significantly altered by mean flow three-dimensionality, especially near the wall, as a result of a reduction in $u'v'$. The eddy viscosity within the 3-D layer is highly anisotropic. In addition, the shear stress vector in the plane of the wall leads and lags the gradient vector in different parts of the flow. The lag of the shear stress vector is mainly due to the residual history of the upstream two-dimensional turbulent boundary layer. The measurements are contrasted with Computations made using the commercial code by FLUENT.

Part I

Two independent experimental investigations of the behavior of turbulent boundary layers with increasing Reynolds number (Re_θ) were recently completed [1]. The experiments were performed in two facilities, the MTL wind tunnel at KTH and the NDF wind tunnel at IIT. While the KTH experiments were carried out on a flat plate, the model used in the NDF was a long cylinder with its axis aligned in the flow direction. Both experiments were conducted in a zero-pressure gradient, covered the range of Reynolds numbers based on the momentum thickness from 2,500 to 27,000, and utilized oil-film interferometry to obtain an independent measure of the wall-shear stress. Contrary to the conclusions of some earlier publications, careful analysis of the data revealed no significant Reynolds number dependence for the parameters describing the overlap region using the classical logarithmic relation. The parameters of the logarithmic overlap region were found to be constant and were estimated to be: $\kappa = 0.38, B = 4.1$.

These two experiments have been recently extended to Reynolds numbers based on momentum thickness exceeding 70,000. The current experiments were also carried out in the National Diagnostic Facility (NDF) at IIT on a 10 m long and 1.5 m wide flat plate using free-stream velocities ranging from 30 to 85 m/s. Again, hot-wire anemometry and oil-film interferometry were used to measure the velocity profiles and the wall-shear stress, respectively. The design of the experiments, and in particular the location and spacing of the velocity profiles in the downstream direction and the hot-wire sensor in the wall-normal direction, developed to facilitate the evaluation of wall-normal *and* streamwise derivatives. The arrangement of the NDF was designed to allow the adjustment of the test-section ceiling to impart various pressure gradients. Several conditions were investigated so far, including: Adverse Pressure Gradient (APG), Zero Pressure Gradient (ZPG), Favorable Pressure Gradient (FPG), Strongly Favorable Pressure Gradient (SFPG), and Complex Pressure Gradient (CPG); displayed in Figure 1.

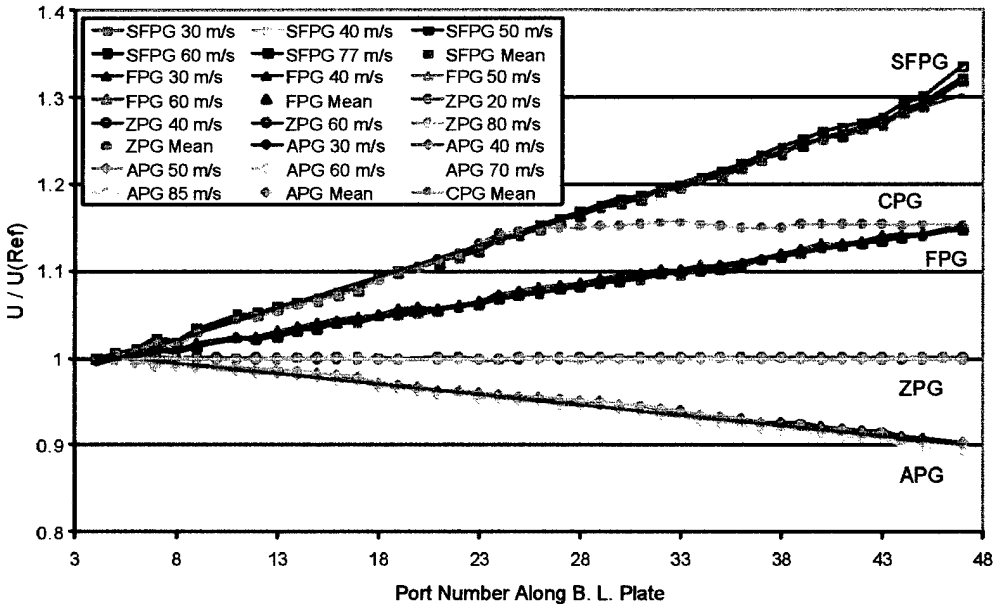

Figure 1: Variation of free-stream velocity along 10-m boundary layer plate for various pressure-gradient conditions.

One of the cornerstones of our approach to measurements of turbulent wall-bounded flows is the *independent* and accurate measurement of the wall shear stress with oil-film interferometry. We believe the only wall-bounded flow that may not require such measurements is the *fully developed* pipe flow, where the careful measurement of pressure gradient can lead to an accurate determination of the friction velocity. For the non-equilibrium boundary layers under various pressure-gradient conditions, one can be dramatically misled by other indirect techniques for the determination of wall-shear stress. Figure 2 compares our recent ZPG measurements with the recent two sets of measurements of Hites and Österlund. The value of the Kárman constant extracted using the correlation proposed by Fernholz [2] and all three sets of data is approximately 0.38. If only our recent data are used the value is 0.373.

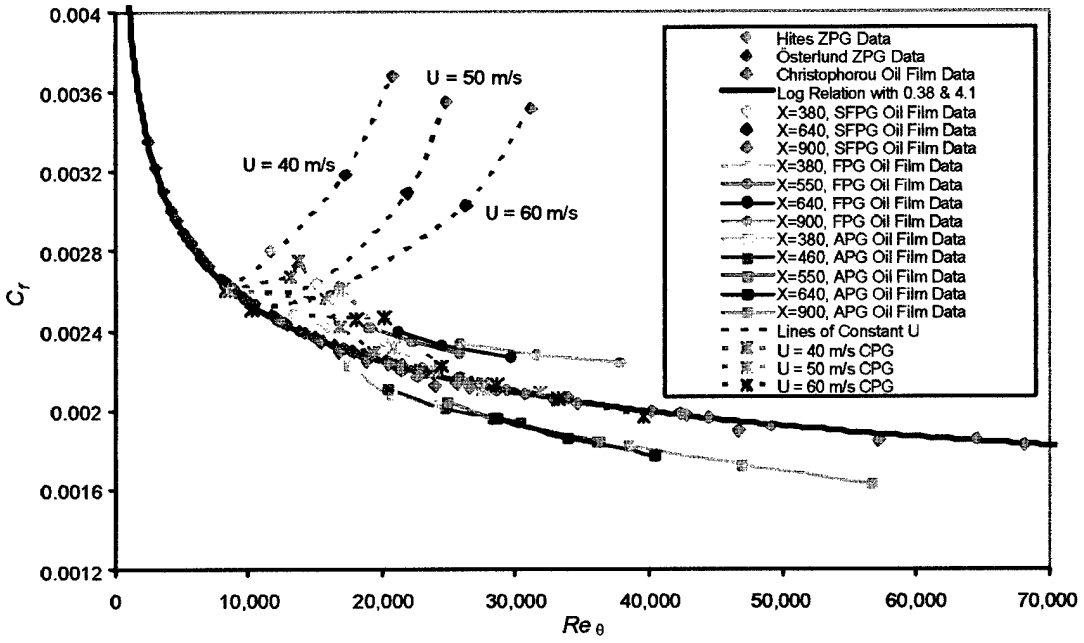

Figure 2: Variation of skin friction with momentum-thickness Reynolds number for different streamwise positions and free-stream velocities.

A few samples of pressure-gradient data are included in Figure 2. In particular, the behaviour of the non-equilibrium layers with the SFPG is most revealing when contrasted to the equilibrium ZPG data where the resulting skin friction is independent of whether Re_θ is varried by changing the free-stream velocity or the downstream distance. As in our earlier work [1], profiles of the mean and rms streamwise component of the velocity and their spatial derivatives are used to examine the effects of the pressure gradient on the inner and outer layers as well as their overlap region. The results demonstrate that the pressure gradient causes significant changes not only in the outer region of the boundary layer but also within the inner region; i.e., the buffer layer. The effect of these changes on Coles' outer layer parameter and the behavior of the maximum turbulence stress have also been documented.

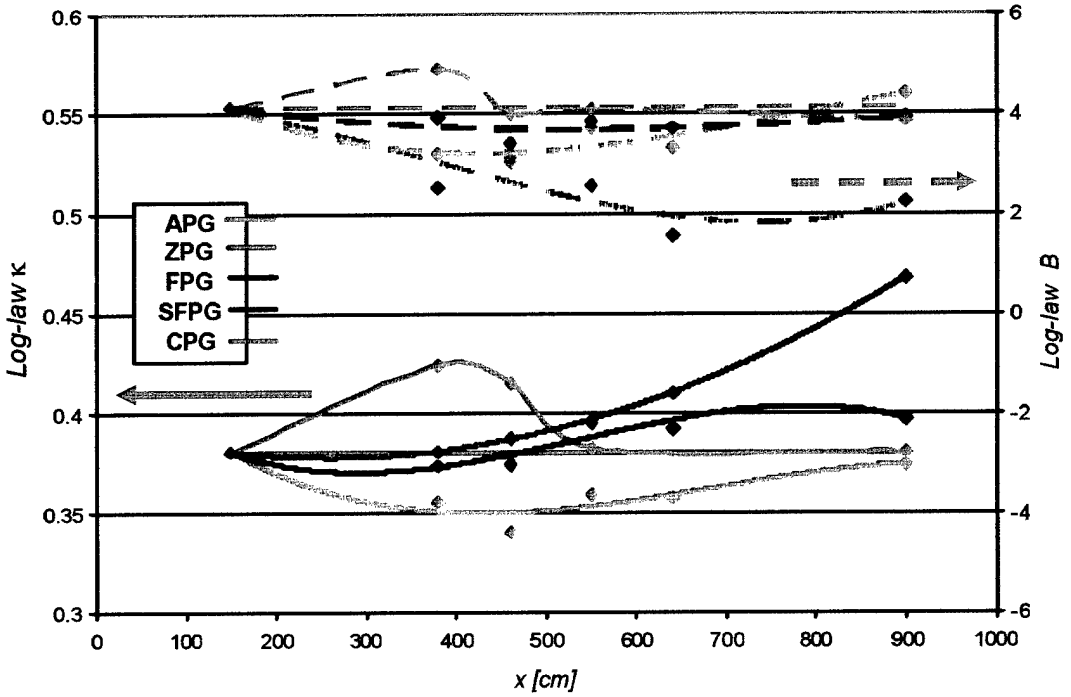

Figure 3: Downstream development of log-law parameters κ and B.

While all of the boundary layers documented exhibit an overlap region accurately represented by a logarithmic law, the values of the log-law parameters are found to vary considerably when the boundary layers are in a state of non-equilibrium; i.e., non self preserving. Figure 3 depicts the variation of these parameters with downstream distance. It appears that when the boundary layers regain their "equilibrium," the Kárman "coefficient" (κ) returns to its established ZPG value of ~ 0.38.

In the case of the SFPG, the extent of the boundary layer plate did not allow us to document the return to equilibrium state. On the other hand, in the case of the Complex Pressure Gradient Condition (CPG), a limited fetch of the same SFPG followed by an adequate distance of a zero pressure gradient, confirms our conjecture regarding the return of the overlap region parameters to their equilibrium values. It should be pointed out, however, that the return of the outer scales of the boundary layer, e.g. as represented by Coles wake parameter Π, is much slower. While the three pressure gradient conditions ZPG, APG and CPG have very similar κ values near the downstream end of the flat plate, the outer scales are largest in the case of the adverse condition and smallest in the CPG case with its strong favourable segment.

A number of yet unexplained differences between wall-bounded turbulent flows in pipes [3], channels [4] and boundary layers are clarified based on the comparison between our measurements in ZPG boundary layers and the present results for different pressure gradients. The variation of the Kárman "coefficient" (κ) from generally accepted values is revealed by these measurements in both equilibrium and non-equilibrium wall-bounded shear flows.

Part II

A three-dimensional turbulent boundary layer over a flat plate has been studied. The 3DTBL is subject to an adverse streamwise pressure gradient as a result of the turning of the flow. This flow field has a two-dimensional equivalent and detailed measurements have been made of the mean flow, pressure gradient, wall shear stress, all six Reynolds stresses and all ten triple velocity correlations. These measurements as well as the simple geometry make it an excellent candidate for testing turbulence models. The mean flow is measured with both a seven-hole probe and a stereo particle image velocimeter. The agreement between all three components of the mean velocity measured by both methods is within the measurement uncertainty. In an effort to overcome the limitations of most of the previous measurements in 3DTBL's available in the literature, the wall shear stress magnitude and the direction were measured with oil-film interferometry, Figure 4.

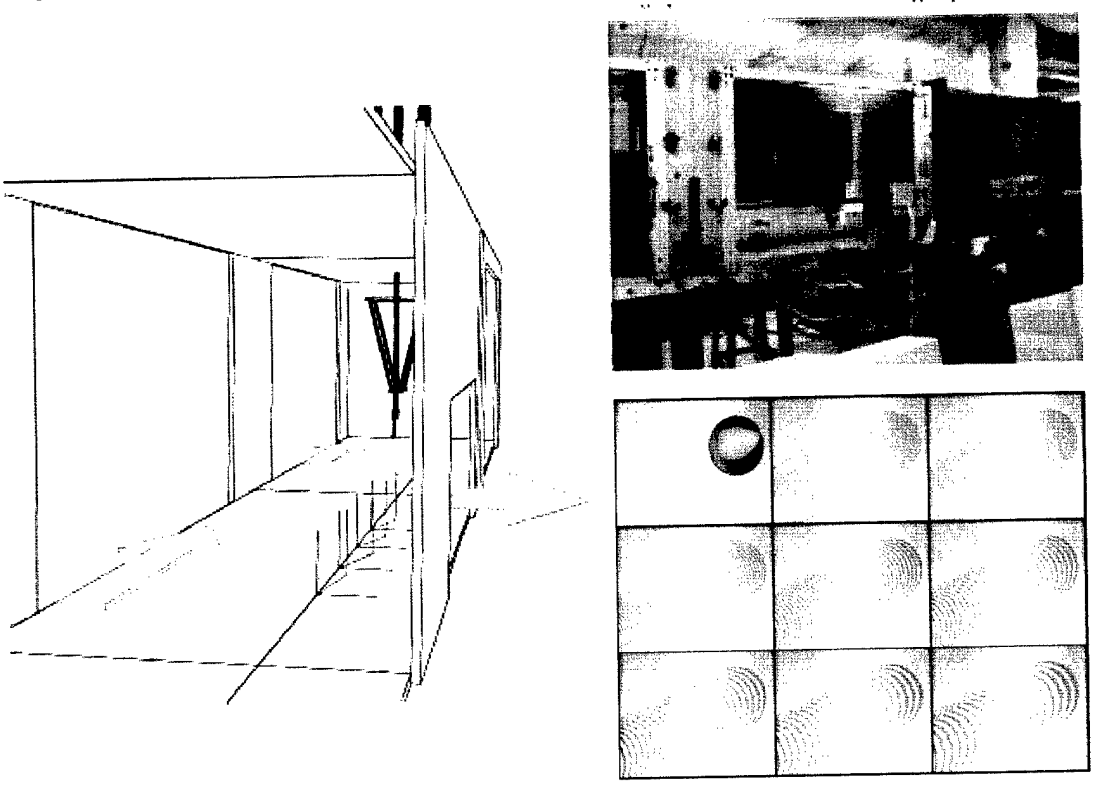

Figure 4: Schematic and photograph of the wind-tunnel test section and images of oil-film interferometry in three-dimensional boundary layer flow.

The mean flow responds, as expected, to the net external forces as shown in Figure 5. The streamwise velocity decelerates continuously at every measurement station and the cross flow increases until station 15 (the flow domain extended over 17 equally-spaced measurement stations) where the wall shear stress begins to dominate and decelerates the cross flow, see Figure 5. The wall shear stress angle increases up to station 9 and then it begins to decrease. Station 9 corresponds to the maximum cross-stream force applied to the flow. The maximum boundary layer skewing is about 16° making this a mildly skewed turbulent boundary layer.

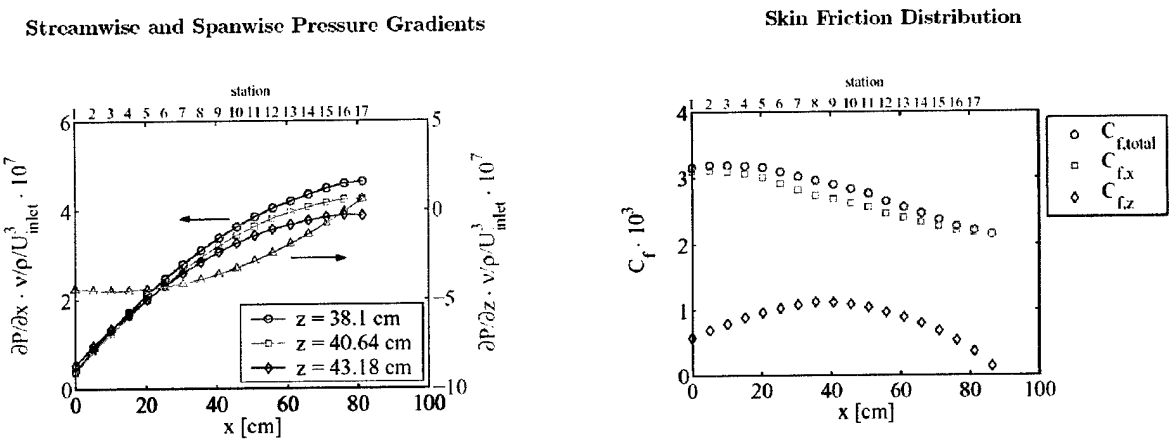

Figure 5: Normalized streamwise and transverse pressure gradients, and total skin-friction coefficient and its streamwise and transverse components.

Downstream Development of $<u'^2>$

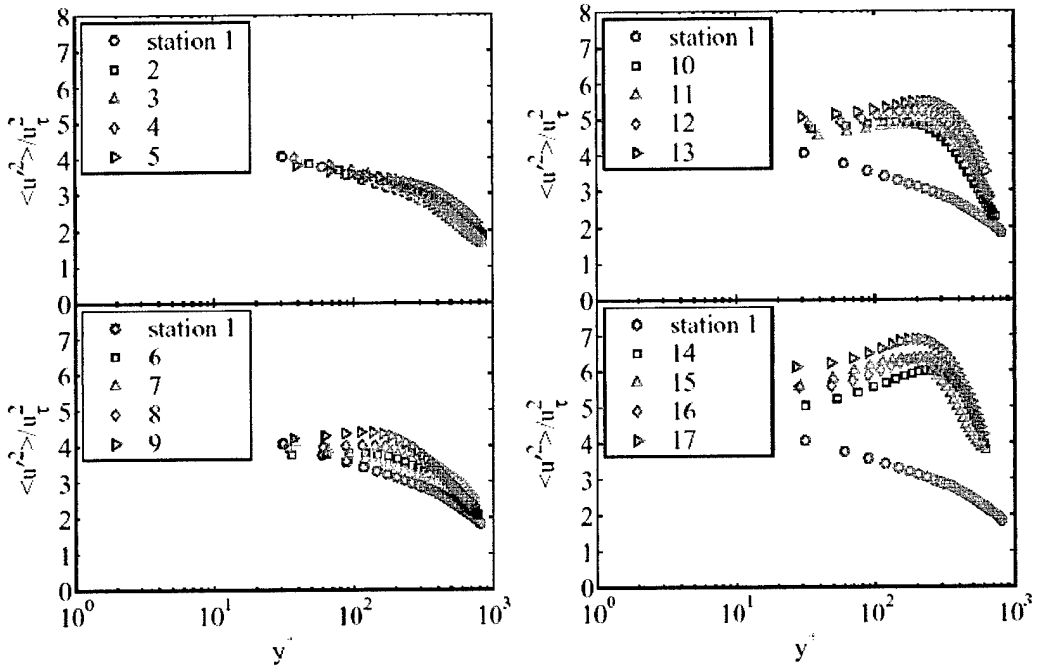

Figure 6: Streamwise and transverse pressure gradient variation along the boundary layer flow normalized by the corresponding wall shear stress component.

The TKE increases slightly over the domain of the three-dimensional flow through changes in $<u'^2>$; see Figure 6. The Reynolds stresses are all affected by the mean flow three-dimensionality. In fact, many of the observed changes in the Reynolds stresses can be attributed to turbulence production with one exception: the Reynolds stress $<w'^2>$ is maintained only by the pressure-rate-of-strain tensor. The pressure-rate-of strain tensor also plays an important role in the dynamics of $<u'^2>$, $<v'^2>$, $<u'v'>$ and $<v'w'>$ near the wall.

Measurements of Townsend's structure parameter indicate that this parameter, which appears frequently in turbulence models, is significantly altered by the mean flow three-dimensionality especially near wall. Values are typically below the 0.15 value reported in 2DTBL's. Reduction in a_1 is mainly attributed to a reduction in $\langle u'v' \rangle$ near the wall. The mixing length is also changed by the three-dimensional mean flow. In the outer part of the boundary layer, $y/\delta > 0.2$, the mixing length is significantly reduced. Near the wall, the proportionality constant which relates the mixing length to the distance from the wall is also changed. This suggests that extensions of mixing length models to 3DTBL's are certain to perform poorly.

Turbulent Viscosity Lead/Lag

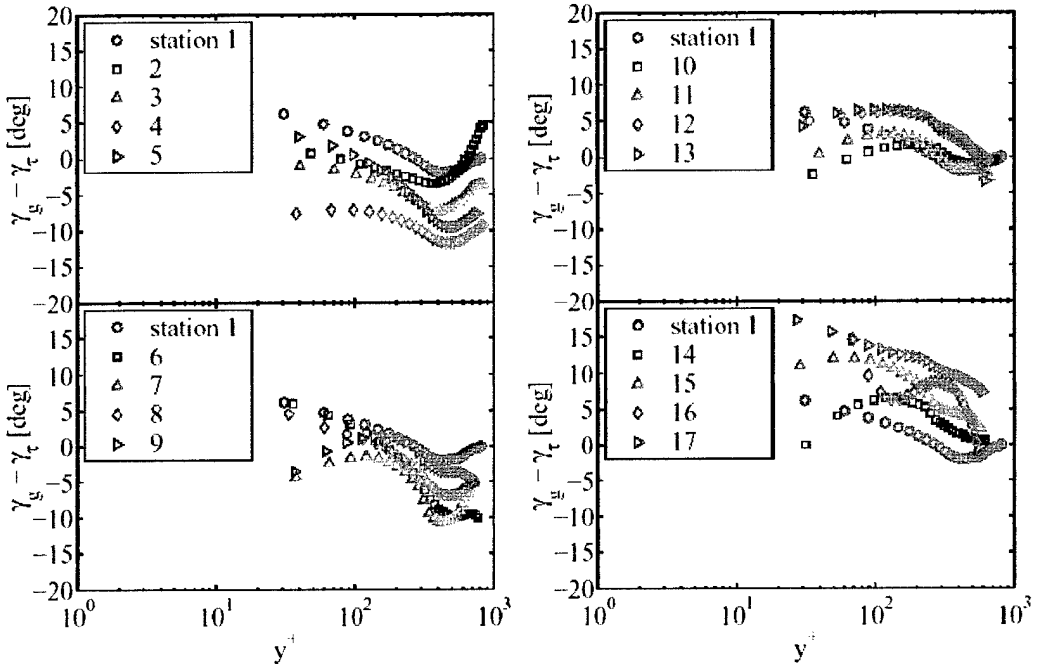

Figure 7: Development along the three-dimensional boundary layer of the streamwise normal stress.

The turbulent eddy viscosity is highly anisotropic and exhibits a very complex behavior. In particular, the turbulent shear stress vector both leads and lags the gradient vector in different parts of the flow, as depicted in Figure 7. The lag of the shear stress vector is mainly due to the residual history of the upstream two-dimensional turbulent boundary layer within the developing 3DTBL. No explanation of the lead is forwarded.

Investigating the turbulent structure of the flow through the two-point velocity correlation indicates that the longitudinal and transverse length scales are changed by the mean flow three-dimensionality in relation to the size of the boundary layer. In most cases, the size of the energy containing eddies decreases with increasing mean flow three-dimensionality except for those responsible for $\langle w^2 \rangle$ which increase in size. Interpretation of this observation leads to the hypothesis that the structure responsible for $\langle u^2 \rangle$ is turned by the secondary flow so that it also produces $\langle w^2 \rangle$.

The joint PDF's of the Reynolds stresses $<u'v'>$, $<v'w'>$ and $<u'w'>$ are analyzed to ascertain how the mean flow three-dimensionality changes the ability of the turbulent motions to produce ejections and sweeps (i.e. positive contributions to the Reynolds stresses). Key results indicate that the ability of the turbulent motions to produce $u'v'$ sweeps is reduced; see Figure 8. In addition, the frequency of quadrant I and quadrant III $v'w'$ motions as well as the frequency of quadrant III $u'w'$ motions are simultaneously increased.

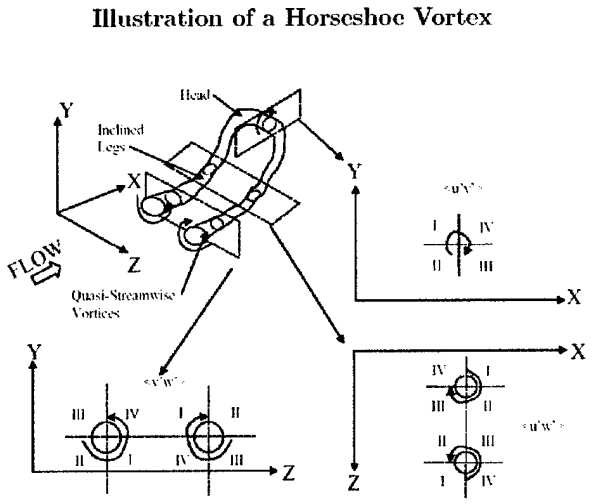

Figure 8: Representation of the relation between the turbulent shear stress vector and the gradient vector in different parts of the flow.

Conditional averaging, as demonstrated in Figure 9, produces turbulent motions consistent with an asymmetric version of the horseshoe/hairpin vortex typically observed in two-dimensional turbulent boundary layers with one exception: the angle of inclination of the legs of the horseshoe vortex can reach as high as 90°. This is much larger than the angle typically reported in two- dimensional turbulent boundary layer studies.

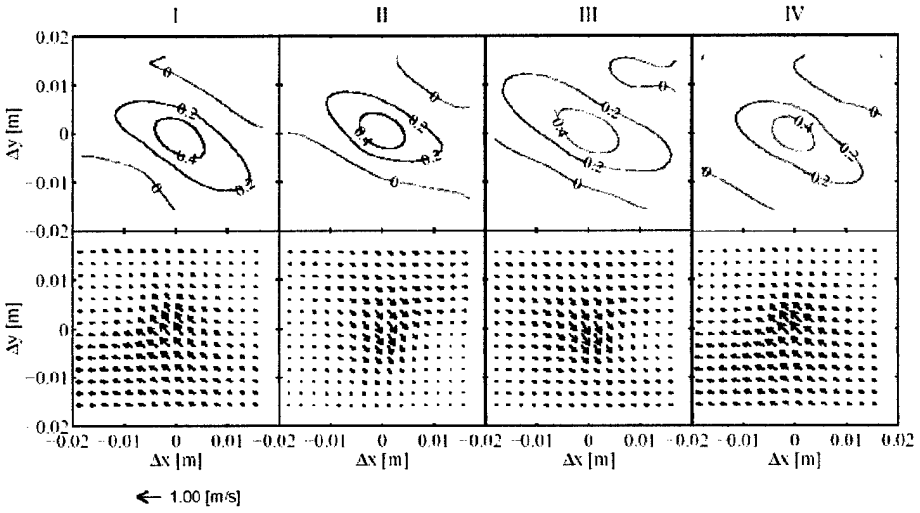

Figure 9: Conditionally averaged $u'w'$ motions downstream in the three-dimensional boundary layer.

Acknowledgment/Disclaimer
This work is sponsored by the Air Force Office of Scientific Research, USAF, under grant number F49620-01-1-0445. The views and conclusions contained herein are those of the authors and should not be interpreted as necessarily representing the official policies or endorsements, either expressed or implied, of the Air Force Office of Scientific Research or the U.S. Government.

References

[1] J.M. Österlund, A.V. Johansson, H. M. Nagib, and M. H. Hites, A note on the overlap region in turbulent boundary layers, Phys. Fluids, 12:1 - 4, 2000.

[2] H. H. Fernholz, Ein halbempirisches Gezetz fuer die Wandreibung in kompressiblen turbulenten Grenzschichten bei isothermer und adiabater Wand. ZAMM, 51: 148 - 149, 1971.

[3] A. E. Perry, S. Hafez, and M. S. Chong, A Possible Reinterpretation of the Princeton Superpipe Data, J. Fluid Mech., v. 439, 2001.

[4] E-S Zanoun, F. Durst, and H. Nagib, Evaluating the law of the wall in two-dimensional, fully-developed turbulent channel flow, Fluids, 15:10 - 3079, 2003.

[5] Steve Gravante, "A Pressure-Driven Three-Dimensional Turbulent Boundary Layer Documented with Stereo Particle Image Velocimetry," PhD thesis, IIT, May 2003.

[6] Ivanka Pelivan, "Computation and Experiments in a Cross-Flow Driven Three-Dimensional Turbulent Boundary Layer," M.S. thesis, IIT, December, 2002.

Personnel Supported

Steve Gravante	Ph. D. Student, Illinois Institute of Technology, Chicago
Chris Christophorou	Ph. D. Student, Illinois Institute of Technology, Chicago
Ivanka Pelivan	M. S. Student, Illinois Institute of Technology, Chicago
Kapil Chauhan	M. S. Student, Illinois Institute of Technology, Chicago
Craig Johnson	Technician, Illinois Institute of Technology, Chicago
Hassan Nagib	Professor, Illinois Institute of Technology, Chicago

Publications

The two thesis listed in the References section have just been completed and several publications are in various stages. The computational M.S thesis by Kapil CHauhan on the same flow field will be available by December 2003 and Chris Christophorou work on measurements at very high Reynolds numbers of two-dimensional boundary layers in presence of pressure gradient effects and transitional wall roughness will appear soon in various manuscroits.

J-D. Ruedi, H. Nagib, J. Österlund and P.A. Monkewitz, "Evaluation of Three Techniques for Wall-Shear Measurements in Three-Dimensional Flows," To appear in Experiments in Fluids, 2003.

J-D. Ruedi, H. Nagib, J. Österlund and P.A. Monkewitz, "Unsteady Wall-Shear Measurements in Boundary Layers Using MEMS," To appear in Experiments in Fluids, 2003.

Hassan Nagib, "The value of wall shear measurements in non-equilibrium or three-dimensional flows, or can we live without them," Workshop on Shear Stress Sensing Techniques and Measurement Results February 5-6, 2004, Caltech, CA, USA.

Hassan Nagib, Chris Christophorou and Peter Monkewitz, "High Reynolds number turbulent boundary layers subjected to various pressure-gradient conditions," IUTAM 2004: One Hundred Years of Boundary Layer Research, Aug. 12-14, 2004; G? ? ngen, Germany

Hassan Nagib, Chris Christophorou, Jean-Daniel Ruedi, Peter Monkewitz, Jens ?fterlund, Steve Gravante, Kapil Chauhan and Ivanka Pelivan, "Can We Ever Rely on Results from Wall-Bounded Turbulent Flows Without Direct Measurements of Wall Shear Stress? (Invited)," AIAA Paper 2004-2392, AIAA Co-Located Conferences, June 2004, Portland, OR.

Honors & Awards Received
None.

AFRL Point of Contact
Dr. Carl P. Tilmann, AFRL/Air Vehicles/Aerodynamic Configuration Branch

Transitions
Continues to interaction with Dr. Spalart at Boeing, and several of Boeing Long Beach and Huntington Beach staff.